

# Electronic Spectrum and Photodissociation of ClONO in Comparison to BrONO

Antonija Lesar,<sup>\*,†</sup> Saša Kovačič,<sup>†</sup> Milan Hodošček,<sup>†,‡</sup> Max Mühlhäuser,<sup>§</sup> and Sigrid D. Peyerimhoff<sup>||</sup>

Department of Physical and Organic Chemistry, Institute Jožef Stefan, Jamova 39, SI-1000 Ljubljana, Slovenia, Centre for Molecular Modeling, National Institute of Chemistry, Hajdrihova 19, SI-1000 Ljubljana, Slovenia, Department of Process Engineering and Environmental Technology, Management Center Innsbruck, Egger-Lienz Strasse 120, A-6020 Innsbruck, Austria, and Institut für Physikalische und Theoretische Chemie der Universität Bonn, Wegelerstrasse 12, 53115 Bonn, Germany

Received: June 16, 2005; In Final Form: September 20, 2005

A theoretical study of the low-lying singlet and triplet states of ClONO is presented. Calculations of excitation energies and oscillator strengths are reported using multireference configuration interaction, MRD-CI, methods with the cc-pVDZ + sp basis set. The calculations predict the dominant transition,  $4^1A' \leftarrow 1^1A'$ , at 5.70 eV. The transition  $2^1A' \leftarrow 1^1A'$ , at 4.44 eV, with much lower intensity nicely matches the experimental absorption maximum observed around 290 nm (4.27 eV). The potential energy curves for both states are found to be highly repulsive along the Cl–O coordinate implying that direct and fast dissociation to the Cl + NO<sub>2</sub> products will occur. Photodissociation along the N–O coordinate is less likely because of barriers on the order of 0.3 eV for low-lying excited states. A comparison between the calculated electronic energies related to the two dominant excited states of ClONO and BrONO indicates that the transitions lie about 0.6 eV higher if bromine is replaced by chlorine. The stratospheric chemistry implications of ClONO and BrONO are discussed.

## I. Introduction

Stratospheric chemistry of chlorine- and nitrogen-containing compounds is important because of their role in the ozone depletion processes. Nitryl chloride, ClNO<sub>2</sub>, and its isomer chlorine nitrite, ClONO, both atmospherically significant molecules<sup>1</sup>, are formally formed by a coupling reaction between the Cl atom and NO<sub>2</sub>. Two reaction products were first identified by Niki et al.<sup>2</sup> in their Fourier transform IR spectroscopic study of the photolysis of a Cl<sub>2</sub>–NO<sub>2</sub> mixture. The preferential formation of the less stable ClONO isomer in the Cl + NO<sub>2</sub> reaction was explained by low-pressure limit rate constant calculations.<sup>3</sup> In 1979, Kawashima<sup>4</sup> confirmed the existence of ClONO and determined the molecular structure of *cis*-ClONO by microwave spectroscopy.

The structural parameters and relative stabilities of ClNO<sub>2</sub> and ClONO isomers have been well studied theoretically. Lee<sup>5</sup> reported the geometry and vibrational frequencies at the coupled cluster CCSD(T) level using a triple- $\zeta$  double-polarized (TZ2P) basis set, while atomic natural orbital (ANO) basis sets of spdfg quality were used in the evaluation of thermochemical quantities. Subsequently, Lee et al.<sup>6</sup> reinvestigated these species by means of various density functional methods and the TZ2P basis set. Recently, Zhu et al.<sup>7</sup> published a B3LYP/6-311+G(3df) study of the potential energy surface of the ClO + NO  $\rightarrow$  Cl + NO<sub>2</sub> reaction and Rice–Ramsperger–Kassel–Marcus (RRKM) calculations of the rate constants for the forward and reverse processes.

The UV absorption cross-sections for ClONO in the gas phase have been investigated over the wavelength range of 230–400 nm,<sup>8</sup> in which the absorption spectrum shows a broad band with a maximum around 290 nm (photoabsorption cross section,  $14.4 \times 10^{-19}$  cm<sup>2</sup>) and a steady increase in intensity below 260 nm. There have been no theoretical studies of the excited states of the ClONO molecule reported in the literature. To aid the assignment of experimentally observed features to transitions to particular electronic excited states for ClONO and to understand its photochemistry, we now report the results of multireference configuration interaction calculations, MRD-CI, of vertical excitation energies for transitions from the ground state to low-lying singlet and triplet states and corresponding oscillator strengths for dipole-allowed processes. The characterization of the nature of the electronic transitions is based on qualitative molecular orbital considerations. Primary photolysis products are predicted from the calculations of the potential energy curves. The most likely UV destruction process leads to Cl + NO<sub>2</sub> or ClO + NO products. Finally, we present a comparison of the low-lying electronic states of ClONO to those of the bromine analogue, BrONO, just recently studied by our group.<sup>9</sup>

## II. Computational Methods

The structural parameters for chlorine nitrite, ClONO, in its ground state were fully optimized using the single- and double-excitation coupled-cluster method (frozen-core approximation), including a perturbation estimate of the effects of connected triple excitations CCSD(T),<sup>10</sup> with the 6-31G(d) basis sets using the Gaussian 03 program package.<sup>11</sup>

The computations of the electronically excited states were performed using a CCSD(T)/6-31G(d) geometry with the multireference single- and double-excitation configuration interaction method MRD-CI implemented in the Diesel program.<sup>12</sup>

\* To whom correspondence should be addressed. Fax: +386 1 251 93 85. E-mail: antonija.lesar@ijs.si.

<sup>†</sup> Institute Jožef Stefan.

<sup>‡</sup> National Institute of Chemistry.

<sup>§</sup> Management Center Innsbruck.

<sup>||</sup> Institut für Physikalische und Theoretische Chemie der Universität Bonn.

The selection of the reference configurations by a summation threshold is carried out automatically. We used a summation threshold of 0.85, which means that the sum of the squared coefficients of all reference configurations selected for each state (root) is above 0.85. The number of reference configurations per irreducible representation (IRREP) was in the range between 20 and 30. An analysis of the molecular orbitals (MO) involved in these selected reference configurations justified the prior choice of treating the 24 valence electrons as active while the remaining electrons were kept in doubly occupied orbitals defined as frozen-core orbitals.

From this set of reference configurations (mains), all single and double excitations in the form of configuration state functions (CSFs) are generated. All configurations of this set with an energy contribution  $\Delta E(T)$  above a given threshold  $T$  were selected, that is, the contribution of a configuration larger than this value relative to the energy of the reference set is included in the final wave function. Selection thresholds of  $T = 5 \times 10^{-7}$  and  $T = 10^{-8}$  hartrees were used for the singlet and triplet states, respectively. The effect of the configurations that contribute less than  $T = 5 \times 10^{-7}$  or  $T = 10^{-8}$  hartrees is accounted for in the energy computation ( $E(\text{MRD} - \text{CI})$ ) by the perturbative  $\lambda$ -extrapolation.<sup>13,14</sup> The contribution of higher excitations is estimated by applying a generalized Langhoff–Davidson correction formula

$$E(\text{MRD} - \text{CI} + Q) = E(\text{MRD} - \text{CI}) - \frac{(1 - c_0^2)[E_{\text{ref}} - E(\text{MRD} - \text{CI})]}{c_0^2}$$

where  $c_0^2$  is the sum of the squared coefficients of the reference species in the total CI wave function and  $E_{\text{ref}}$  is the energy of the reference configurations.

We computed four singlet and four triplet states per IRREP for CIONO of  $C_s$  symmetry. The number of CSFs directly included in the energy calculations are as large as 1.3 million and 1.5 million for the singlet and triplet, respectively, selected from a total space of 3.5 million and 4.5 million generated configurations, respectively. For the calculations of excited states, we used the correlation-consistent AO basis set of Dunning of double- $\zeta$  quality.<sup>15,16</sup> In addition, the basis set was enlarged by a s-Rydberg function located at the nitrogen and by a negative ion function for the chlorine atom, thus giving the cc-pVDZ+sp basis set. The exponents taken are  $\alpha_s(\text{N}) = 0.028$  and  $\alpha_p(\text{Cl}) = 0.049$ . Double- $\zeta$  quality of the basis set was considered adequate for the species of interest. From our recent studies on halogen–nitrogen oxide compounds,<sup>9,17,18</sup> it is evident that the calculated excitation energies can have an error on the order of 0.3 eV.

For the investigation of the photodissociation pathways of CIONO, two models were considered. In the first model, the Cl–O bond length of the ground-state CIONO was changed stepwise in the range from 1.70 to 10 Å, while all other geometrical parameters were optimized at the CCSD(T)/6-31G(d) level of theory. In the second model, the potential energy curves were obtained by elongating the ClO–NO bond length stepwise from 1.33 to 10 Å. Again, all other bond lengths and angles were optimized.

### III. Results and Discussion

The ground electronic state of CIONO is a singlet state of  $C_s$  symmetry,  $1^1A'$ , with 12 doubly occupied valence orbitals. The equilibrium geometry was optimized at the CCSD(T)/6-31G(d) level and is presented in Figure 1. This level of calculation is of sufficient accuracy to predict a reliable geometry, as can

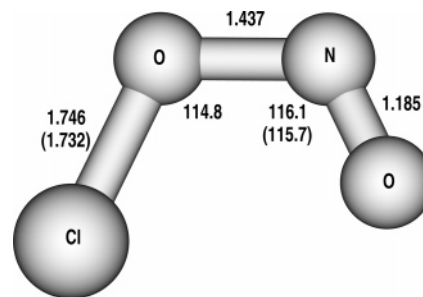


**Figure 1.** CCSD(T)/6-31G(d) equilibrium geometry of chlorine nitrite, *cis*-CIONO, with the vibrationally averaged data determined from experiments<sup>4</sup> in parentheses. The bond lengths are given in angstroms and bond angles in degrees.

**TABLE 1: Calculated Vertical Excitation Energies  $\Delta E$  (eV) and Oscillator Strengths  $f$  to Singlet Excited States of CIONO<sup>a</sup>**

| state    | excitation             | CIONO      |        |                            |                           | BrONO      |        |                            |                           |
|----------|------------------------|------------|--------|----------------------------|---------------------------|------------|--------|----------------------------|---------------------------|
|          |                        | $\Delta E$ | $f$    | $\Delta E_{\text{trip}}^b$ | $\Delta E_{\text{exp}}^c$ | $\Delta E$ | $f$    | $\Delta E_{\text{trip}}^b$ | $\Delta E_{\text{exp}}^d$ |
| $1^1A'$  | $(9a')^2(3a'')^2$      | 0.00       | 0      |                            |                           | 0.00       | 0      |                            |                           |
| $1^1A''$ | $9a' \rightarrow 4a''$ | 4.09       | 0.003  | 3.27                       |                           | 3.76       | 0.002  | 2.97                       |                           |
| $2^1A'$  | $3a' \rightarrow 4a''$ | 4.44       | 0.004  | 4.53 <sup>e</sup>          | 4.27 <sup>g</sup>         | 3.88       | 0.018  | 3.68                       | 3.92                      |
|          | $9a' \rightarrow 10a'$ |            |        |                            |                           |            |        |                            |                           |
| $2^1A''$ | $3a' \rightarrow 10a'$ | 4.79       | 0.0003 | 4.09                       |                           | 4.07       | 0.0002 | 3.50                       |                           |
| $3^1A'$  | $8a' \rightarrow 10a'$ | 5.33       | 0.003  | 4.72                       |                           | 4.45       | 0.0003 | 3.81                       |                           |
| $3^1A''$ | $8a' \rightarrow 4a''$ | 5.96       | 0.0001 | 6.03                       |                           | 5.18       | 0.0    | 5.16                       |                           |
| $4^1A'$  | $9a' \rightarrow 10a'$ | 5.70       | 0.155  | 4.76 <sup>f</sup>          |                           | 5.13       | 0.125  | 4.51                       | 5.44                      |
|          | $3a' \rightarrow 4a''$ |            |        |                            |                           |            |        |                            |                           |
| $4^1A''$ | $2a' \rightarrow 10a'$ | 7.14       | 0.001  | 6.83                       |                           | 5.92       | 0.001  | 5.64                       |                           |

<sup>a</sup> The MO notation classifies the 24 valence electrons active in the calculations. <sup>b</sup>  $\Delta E_{\text{trip}}$  is the excitation energy of the corresponding triplet transitions relative to the ground-state  $1^1A'$  energy. <sup>c</sup> From ref 8. <sup>d</sup> From ref 19. <sup>e</sup>  $9a' \rightarrow 10a'$ , single electron transition. <sup>f</sup>  $3a' \rightarrow 4a''$ , single electron transition. <sup>g</sup> Approximate maximum in a broad absorption feature.

be proven from a comparison with the experimental values,<sup>4</sup> which are stated in parentheses in the figure. At the CCSD(T)/6-31G(d) level, the relative energy of the *cis* against the *trans* isomer is only 3.5 kcal mol<sup>-1</sup> and the energy barrier for *cis*–*trans* isomerization is 12.7 kcal mol<sup>-1</sup>. Although the 6-31G(d) basis set is rather small, the calculated *cis*–*trans* energy difference is in reasonable accord with the previously reported value of  $3.1 \pm 0.8$  kcal mol<sup>-1</sup> obtained at CCSD(T)/TZ2P.<sup>5</sup> Recent calculations at the CCSD(T)/6-311+G(3df)//B3LYP/6-311+G(3df) level of theory performed by Zhu and Lin<sup>7</sup> predict that the *cis* conformation is 3.9 kcal mol<sup>-1</sup> lower in energy than the *trans* form and find an energy barrier of 12.0 kcal mol<sup>-1</sup>.

**Electronic Spectrum of CIONO.** We first examine the vertical excitation energies and oscillator strengths of *cis*-CIONO, which are very useful to explain its UV spectra. The excited states up to about 7 eV are included; higher states are considered to be unimportant in the view of stratospheric photochemistry. The results of the calculations at the MRD-CI level using the cc-pVDZ + sp basis set and the available experimental values are summarized in Table 1 together with related values for *cis*-BrONO for the subsequent comparison. We also include the corresponding triplet excitations. In Figure 2, we present the SCF-MO energy scheme of valence orbitals of CIONO, and in Figure 3, the charge density contours of some important valence ( $7a'$ ,  $8a'$ ,  $9a'$ ,  $2a''$ ,  $3a''$ ) and virtual ( $10a'$ ,  $4a''$ ) orbitals are shown. In our coordinate system, the  $y$  axis is along the N–O terminal bond and the other oxygen and chlorine atoms lie in the  $yx$  plane.

The ground-state electronic configuration is  $(9a')^2(3a'')^2$  with regard to the 24 valence electrons treated as active in the CI

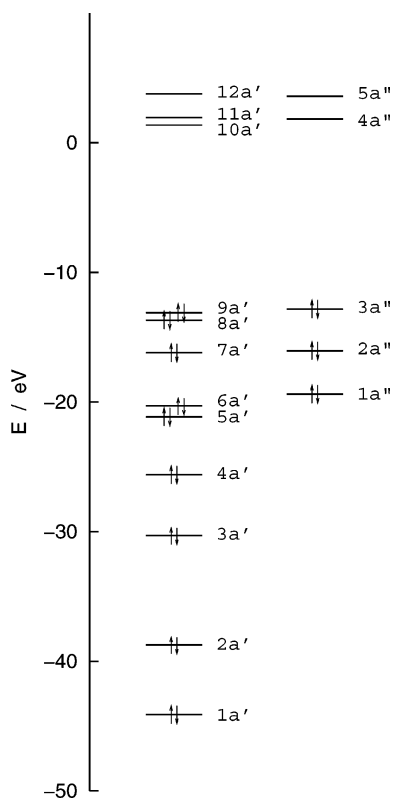


**Figure 2.** Schematic diagram of the molecular orbital energy spectrum of the ground-state configuration of *cis*-ClONO,  $C_s$  symmetry, obtained at the SCF level.

calculations. As can be seen from Table 1, the lowest dipole-allowed excitation (HOMO–LUMO) is computed at 4.09 eV ( $9a' \rightarrow 4a''$ ). The next low-energy state has a different symmetry,  $2^1A'$ , at 4.44 eV, and shows a multireference character, representing linear combinations of  $3a'' \rightarrow 4a''$  and  $9a' \rightarrow 10a'$ . Both transitions ( $1^1A' \leftarrow X^1A'$ ,  $f = 0.003$  and  $2^1A' \leftarrow X^1A'$ ,  $f = 0.004$ ) have comparable oscillator strengths  $f$ . It is quite conceivable that both transitions contribute to the measured broad (260 to 400 nm) absorption spectrum<sup>8</sup> that shows a maximum between 4.24 eV (290 nm) and 4.35 eV (285 nm) and additional structures in the range below 4.0 eV (310 nm).

The nature of the first transition,  $9a' \rightarrow 4a''$ , is from an in-plane orbital to one perpendicular to the plane, accompanied by charge transfer from the in-plane  $\pi^*(\text{Cl}-\text{O})$  to the perpendicular  $\pi^*(\text{N}-\text{O})$ , explaining the relatively low intensity. In the  $2^1A' \leftarrow X^1A'$  transition, the dominant in-plane  $9a' \rightarrow 10a'$  term is in principle expected to lead to considerable  $f$  values but Figure 3 shows that the  $9a'$  orbital has large contributions from  $\text{Cl}(p_x)$  while  $\text{Cl}(p_y)$  is dominant in  $10a'$ , that is, an approximate atomic situation, which leads to a relatively low  $9a' \rightarrow 10a'$  transition probability.

By far the strongest transition is found at 5.70 eV with  $f = 0.155$ . The upper state possesses the complementary character of  $2^1A'$ . The  $f$  value is large because both the (initial)  $3a''$  and (final)  $4a''$  orbitals possess their maximum density above and below the molecular plane and the transition  $3a'' \rightarrow 4a''$  can be considered as a charge transfer from  $n$  and  $\pi^*(\text{Cl}-\text{O})$  of  $3a''$  to  $\pi^*(\text{N}-\text{O})$  of  $4a''$ .

The transitions  $3a'' \rightarrow 10a'$  and  $8a' \rightarrow 4a''$ , calculated at 4.79 and 5.96 eV, respectively, are expected to be weak since the corresponding MOs fall onto perpendicular planes. Again, the finding that MO  $2a''$  represents  $\pi$ -bonding along  $\text{Cl}-\text{O}$  and  $\text{N}-\text{O}$  linkages in perpendicular planes compared to MO  $10a'$  plus some charge transfer is in line with a rather small  $f$  value

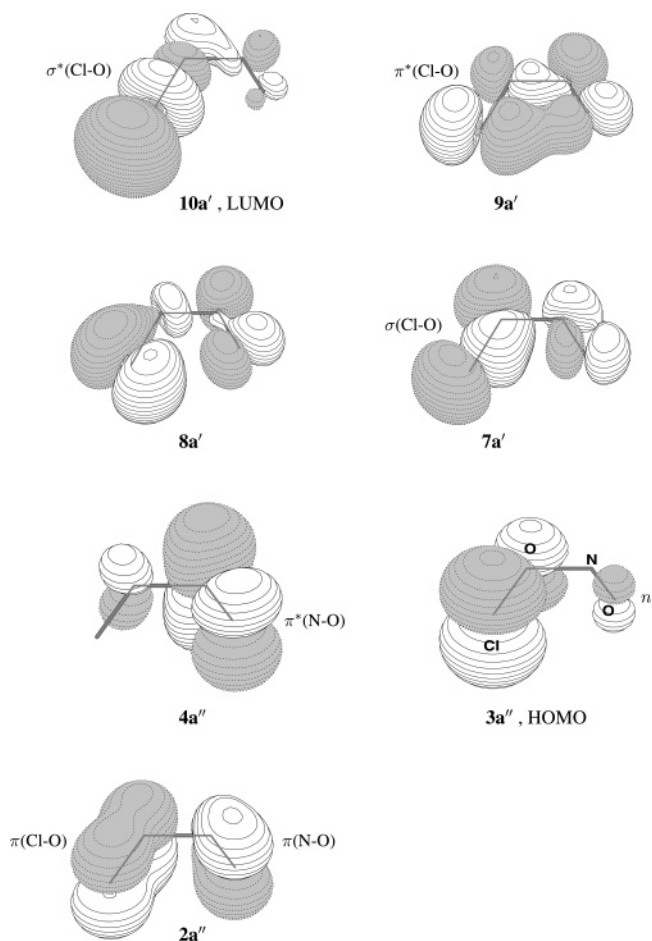


**Figure 3.** Charge density contours of characteristic occupied valence orbitals ( $7a'$ ,  $8a'$ ,  $9a'$ ,  $2a''$ ,  $3a''$ ) and the lowest unoccupied molecular orbitals ( $10a'$ ,  $4a''$ ) of *cis*-ClONO.

of 0.001 for  $2a'' \rightarrow 10a'$ . MO  $7a'$  represents  $\sigma(\text{Cl}-\text{O})$ , while  $4a''$  shows no electronic density at the chlorine center.

The electronic transitions from the ground state of ClONO to the singlet excited states are most likely processes involved in the photoinduced transitions and dissociations because of spin conservation. Although a singlet  $\rightarrow$  triplet transition is considered to be forbidden due to the different spin, such a transition could occur if there is significant spin–orbital coupling. The presence of the heavy chlorine atom in ClONO might assist in this case. Recent photodissociation experimental studies have revealed that for  $\text{HOBr}$ ,<sup>20,21</sup>  $\text{HOCl}$ ,<sup>21</sup> and  $\text{NOCl}$ <sup>22</sup> the spin–orbit coupling is strong enough to allow a weak transition to the triplet states. Thus, we have also considered the vertical excitation energy for the lowest triplet excited state; these values are given in Table 1. An inspection of Table 1 demonstrates that the triplet states are computed to be about 0.3 to 0.8 eV below the corresponding singlet states, with the exceptions of  $2^3A'$ ,  $4^3A'$ , and  $3^3A''$ . Such relatively large singlet–triplet splitting corresponds to typical valence-type transitions as discussed above. The  $2^3A'$  and  $4^3A'$  are found to be single-configuration states, in contrast to their singlet counterparts. Due to configuration mixing of  $9a' \rightarrow 10a'$  and  $3a'' \rightarrow 4a''$ , the energy of  $2^1A'$  falls below that of  $2^3A'$  ( $9a' \rightarrow 10a'$ ) and the energy of  $4^3A'$  is markedly shifted upward relative to the single-configuration  $3a'' \rightarrow 4a''$  configuration state. The fact that  $3^3A''$  ( $8a' \rightarrow 4a''$ ) is computed slightly above  $3^1A''$  is simply an artifact of the calculations, which treat singlets and triplets in different secular equations. It is evident from Figure 3 that  $4a''$  shows no Rydberg contribution. Nevertheless, the singlet–triplet

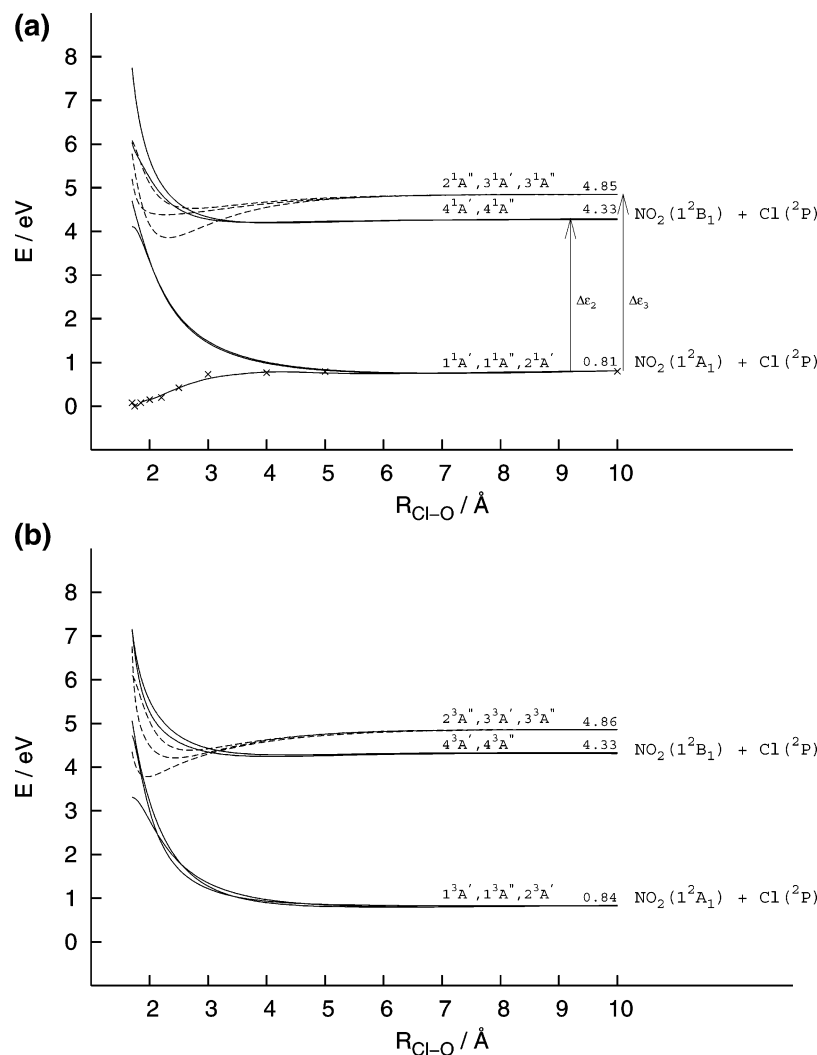


**Figure 4.** Calculated MRD-CI potential energy curves of the low-lying states of the *cis*-CIONO along a fragmentation pathway breaking the Cl–O bond: (a) singlet states,  $\Delta\epsilon_i$  illustrates the energy difference between two dissociation channels, and (b) triplet states.

splitting of these  $3A''$  states is expected to be small since the overlap between the upper and lower orbitals—which are dominant contributions in the respective exchange integral—is presumably small. Numerous calculations employing different basis sets and, in addition, CI calculations using an active space concept instead of the described selection of reference configurations place the  $3^3A''$  state between 5.7 and 6.0 eV. As a consequence, this difference gives a value of the error margin of the present calculations.

**Potential Energy Curves for CIONO.** The potential energy curves along the reaction coordinates Cl–ONO and ClO–NO are presented in Figures 4 and 5, respectively. The ground state,  $X^1A'$ , is bound, while both important transitions  $2^1A' \leftarrow X^1A'$  (4.44 eV) and  $4^1A' \leftarrow X^1A'$  (5.70 eV) lead to repulsive states along the Cl–O coordinate. This is in accordance with our simple MO picture that the populated  $4a''$  is nonbonding for Cl–O while MO  $10a'$  is  $\pi^*$  antibonding. Consequently, the population of this  $\pi^*$  type (Cl–O) antibonding MO  $10a'$  will lead to the dissociation of the Cl–O linkage. Thus, the molecule CIONO might be formed during polar night, while photoinduced dissociation into Cl and  $\text{NO}_2$  during the day is very likely. The energy calculated for the second dissociation channel is in a reasonable agreement with the experimentally measured value for the second low-lying excited state of  $\text{NO}_2$ . While our present computations place  $\Delta\epsilon_2$  at 3.5 eV, the experimental value is

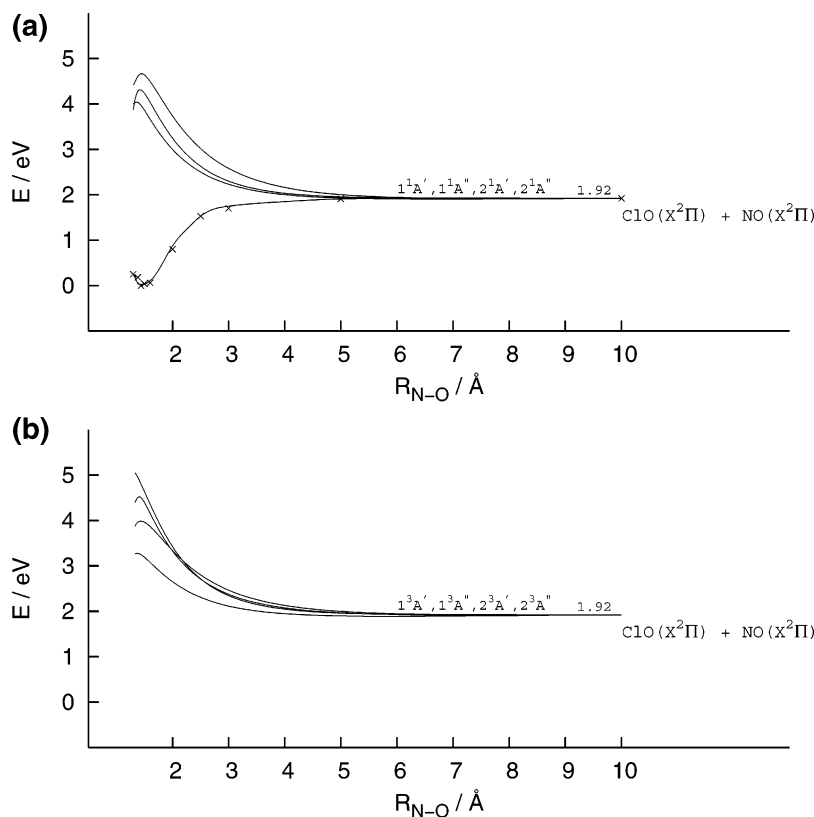
3.2 eV.<sup>23</sup> Furthermore, the dissociation channels of the triplets are in accordance with the corresponding singlets to about 0.03 eV.

Figure 5 indicates that the dissociation along the N–O coordinate is less probable. The potential energy curves of the low-lying excited states show barriers up to about 0.3 eV. Photofragmentation breaking the N–O bond has to overcome this small barrier. Singlet and triplet curves lead to the same dissociation channel at 1.92 eV which corresponds to the ground-state fragments  $\text{NO}(X^2\Pi) + \text{ClO}(X^2\Pi)$ .

**Comparison of the CIONO and BrONO Low-Lying Excited States.** It is interesting to note the UV spectral similarity between CIONO and BrONO. The absorption spectrum of the bromine analogue has been studied by both experiment<sup>8</sup> and ab initio calculations,<sup>9</sup> in which MRD-CI vertical excitation energies for the cc-pVTZ + sp basis set are reported. For a reliable comparison with CIONO, we present in Table 1 the values for BrONO calculated with the cc-pVDZ + sp basis set. We should emphasize that the energies obtained with the basis set of double- $\zeta$  quality are within about 0.1 eV of those resulting from calculations with the triple- $\zeta$  basis set.<sup>9</sup>

The computed excitation energies of *cis*-BrONO nicely match the absorption peaks in the experimental spectrum recorded in the range of 200–365 nm.<sup>8</sup> The intense absorption band located at 228 nm (5.44 eV) coincides with the computed vertical energy





**Figure 5.** Calculated MRD-CI potential energy curves of the low-lying states of the *cis*-ClONO along a fragmentation pathway breaking the N–O bond: (a) singlet states and (b) triplet states.

of 5.13 eV for the  $4^1A'$  state having a large oscillator strength. The low-intensity broad band centered around 316 nm (3.92 eV) agrees with the calculated transition energy of 3.88 eV for the  $2^1A'$  state. The near UV absorption spectrum of chlorine nitrite in the wavelength range of 230–400 nm<sup>8</sup> showed the low-intensity broad band centered around 290 nm (4.27 eV), which is consistent with the computed values of 4.44 eV. At 5.70 eV, a remarkably strong transition is computed; thus, the strong increase of absorption below the lower limit of measurements with a maximum around 218 nm is predicted from the calculations presented in this work.

The calculated electronic transition for the first singlet excited state,  $1^1A''$ , of ClONO (4.09 eV) is 0.33 eV higher in energy than that for BrONO (3.76 eV), thus, the transition is red shifted by 26 nm if bromine is replaced by chlorine. The vertical excitation energies for both the important  $2^1A'$  and  $4^1A'$  states of ClONO (4.44 and 5.70 eV, respectively) are higher by 0.56 eV relative to the corresponding states for the BrONO species (3.88 and 5.13 eV, respectively). Actually, an examination of electronic spectra for chlorine and bromine nitrites in Table 1 shows that all low-lying electronic transitions are red shifted; the shift lies between 0.3 and 1.2 eV. The red shift in electronic transition upon bromination has been recently reported for HOOCl and HOOBr compounds.<sup>24</sup> The first triplet excited state of ClONO is calculated at 3.27 eV (379 nm) above the ground state and is 0.8 eV lower than the first singlet excited state. In BrONO, the analogous triplet transition is located at 2.97 eV (418 nm) and the triplet–singlet difference is again 0.8 eV.

Photofragmentation of ClONO and BrONO shows a similar behavior. Low-lying excited states of both compounds are highly repulsive in the X–N coordinate, implying direct and fast photodissociation to NO<sub>2</sub> and halogen atoms rather than via the N–O coordinate leading to NO and OX fragments.

In conclusion, the atmospheric implications are given. Bromine nitrite has more states that are accessible to the solar radiation in the lower stratosphere than its chlorine analogue. For ClONO, the  $1^1A''$ ,  $1^3A''$ , and eventually  $2^1A'$  states at 4.09, 3.27, and 4.44 eV, respectively, will be accessible, while for BrONO, there are four singlet and four triplet low-lying states accessible for solar radiation. These states are all of the states up to  $3^1A'$  and  $3^3A'$ . Our results suggest that the ClONO or BrONO species may not be considered as a chlorine or bromine stratospheric reservoir species under sunlight conditions.

#### 4. Summary

Vertical excitation energies for the low-lying singlet and triplet electronic states have been calculated for the ClONO molecule using ab initio MRD-CI methods with the double- $\zeta$  correlation-consistent basis set enlarged by s(N) and p(Cl) long-range functions.

The dominant transition in the electronic spectrum of *cis*-ClONO is located at 5.70 eV ( $4^1A' \leftarrow X^1A'$ ) with strong intensity. This transition shows multireference character, representing linear combinations of  $3a'' \rightarrow 4a''$  and  $9a' \rightarrow 10a'$  and is considered as a  $n(O)$ ,  $\pi^*(Cl-O) \rightarrow \pi^*(N-O)$ , and in-plane  $\pi^* \rightarrow \sigma^*(Cl-O)$  type transition, respectively. The similar multireference character also corresponds to the transition calculated at 4.44 eV ( $2^1A' \leftarrow X^1A'$ ), but its intensity is relatively low. The calculated excitation energy is in good agreement with the low-intensity broad band centered around 290 nm (4.27 eV) observed in the experimental spectrum.<sup>8</sup> Also, an increase of absorption below 250 nm supports our prediction that the intense transition in the spectrum should appear around 220 nm (5.7 eV). Both important transitions lead to states that are strongly repulsive along the Cl–O coordinate and show that

CIONO undergoes dissociation forming the Cl and NO<sub>2</sub> products. ClO + NO products are less probable due to the energy barrier along the N–O coordinate.

When the first dipole-allowed electronic transitions of CIONO (4.09 eV) and BrONO (3.76 eV) are compared, it is seen that the transition in the chlorine analogue lies only 0.33 eV higher than that in the bromine compound. Further, the vertical excitation energies for the prominent 2<sup>1</sup>A' and 4<sup>1</sup>A' states are somewhat higher (0.56 and 0.57 eV, respectively) for CIONO than the corresponding energies for BrONO. Low-lying excited states of both compounds are highly repulsive in the X–N coordinate, implying direct and fast photodissociation to NO<sub>2</sub> and halogen atoms rather than via the N–O coordinate leading to NO and OX fragments. Atmospheric implications of these results suggest that the CIONO or BrONO species may not be considered as a chlorine or bromine stratospheric reservoir species under sunlight conditions.

**Acknowledgment.** This work was funded by the Ministry of Science of Slovenia, program Grant No. P2-0148, and partly by the Slovenian-Austrian bilateral, project Grant No. SI-AT/04-05/20.

## References and Notes

- (1) DeMore, W. B.; Sander, S. P.; Golden, D. M.; Hampson, R. F.; Kurylo, M. J.; Howard, C. J.; Ravishankara, A. R.; Kolb, C. E.; Molina, M. J. *NASA JPL Publ. 92-20*, **1992**, Evaluation 10.
- (2) Niki, H.; Maker, P. D.; Savage, C. M.; Breitenbach, L. P. *Chem. Phys. Lett.* **1978**, *59*, 78.
- (3) Cheng, J. S.; Baldwin, A. C.; Golden, D. M. *J. Chem. Phys.* **1979**, *71*, 2021.
- (4) Kawashima, Y.; Takeo, H.; Matsumura, C. *Chem. Phys. Lett.* **1979**, *63*, 119.
- (5) Lee, T. J. *J. Phys. Chem.* **1994**, *98*, 111.
- (6) Lee, T. J.; Bauschliker, C. W., Jr.; Jayatilaka, D. *Theor. Chem. Acc.* **1997**, *97*, 185.
- (7) Zhu, R. S.; Lin, M. C. *ChemPhysChem* **2004**, *5*, 1864.
- (8) Molina, L. T.; Molina, M. J. *Geophys. Res. Lett.* **1977**, *4*, 83.
- (9) Lesar, A.; Kovačič, S.; Hodošček, M.; Stadler, M. G.; Mühlhäuser M.; Peyerimhoff, S. D. *Mol. Phys.* **2005**, in press.
- (10) Pople, J. A.; Gordon, M. H.; Raghavachari, K. *J. Chem. Phys.* **1987**, *87*, 5968.
- (11) Frisch, M. J.; Trucks, G. W.; Schlegel, H. B.; Scuseria, G. E.; Robb, M. A.; Cheeseman, J. R.; Montgomery, J. A., Jr.; Vreven, T.; Kudin, K. N.; Burant, J. C.; Millam, J. M.; Iyengar, S. S.; Tomasi, J.; Barone, V.; Mennucci, B.; Cossi, M.; Scalmani, G.; Rega, N.; Petersson, G. A.; Nakatsuji, H.; Hada, M.; Ehara, M.; Toyota, K.; Fukuda, R.; Hasegawa, J.; Ishida, M.; Nakajima, T.; Honda, Y.; Kitao, O.; Nakai, H.; Klene, M.; Li, X.; Knox, J. E.; Hratchian, H. P.; Cross, J. B.; Bakken, V.; Adamo, C.; Jaramillo, J.; Gomperts, R.; Stratmann, R. E.; Yazyev, O.; Austin, A. J.; Cammi, R.; Pomelli, C.; Ochterski, J. W.; Ayala, P. Y.; Morokuma, K.; Voth, G. A.; Salvador, P.; Dannenberg, J. J.; Zakrzewski, V. G.; Dapprich, S.; Daniels, A. D.; Strain, M. C.; Farkas, O.; Malick, D. K.; Rabuck, A. D.; Raghavachari, K.; Foresman, J. B.; Ortiz, J. V.; Cui, Q.; Baboul, A. G.; Clifford, S.; Cioslowski, J.; Stefanov, B. B.; Liu, G.; Liashenko, A.; Piskorz, P.; Komaromi, I.; Martin, R. L.; Fox, D. J.; Keith, T.; Al-Laham, M. A.; Peng, C. Y.; Nanayakkara, A.; Challacombe, M.; Gill, P. M. W.; Johnson, B.; Chen, W.; Wong, M. W.; Gonzalez, C.; Pople, J. A. *Gaussian 03*, revision B.03; Gaussian, Inc.: Wallingford, CT, 2004.
- (12) Hanrath, M.; Engels, B. *Chem. Phys.* **1997**, *225*, 197.
- (13) Buenker, R. J.; Peyerimhoff, S. D. *Theor. Chim. Acta* **1974**, *35*, 33.
- (14) Buenker, R. J.; Peyerimhoff, S. D. *Theor. Chim. Acta* **1975**, *39*, 217.
- (15) Dunning, T. H., Jr. *J. Chem. Phys.* **1989**, *90*, 1007.
- (16) Woon, D. E.; Dunning, T. H., Jr. *J. Chem. Phys.* **1993**, *98*, 1358.
- (17) Lesar, A.; Hodošček, M.; Mühlhäuser, M.; Peyerimhoff, S. D. *Chem. Phys. Lett.* **2004**, *383*, 84.
- (18) Lesar, A.; Kovačič, S.; Hodošček, M.; Mühlhäuser M.; Peyerimhoff, S. D. *J. Phys. Chem. A* **2004**, *108*, 9469.
- (19) Burkholder, J. B.; Orlando, J. J. *Chem. Phys. Lett.* **2000**, *317*, 603.
- (20) Barnes, R. J.; Lock, M.; Coleman, J.; Sinha, A. *J. Phys. Chem.* **1996**, *100*, 453.
- (21) Francisco, J. S.; Hand, M. R.; Williams, I. H. *J. Phys. Chem.* **1996**, *100*, 9250.
- (22) Bay, Y. Y.; Qian, C. X. W.; Iwata, I.; Segal, G. A.; Reisler, H. *J. Chem. Phys.* **1989**, *90*, 3903.
- (23) Douglas, A. E.; Huber, K. P. *Can. J. Phys.* **1964**, *43*, 74.
- (24) Francisco, J. S.; Hand, M. R.; Williams, I. H. *J. Chem. Phys.* **2000**, *112*, 8483.